**IRAQI BULLETIN OF GEOLOGY AND MINING (IBGM)\
IRAQ GEOLOGICAL SURVEY (GEOSURV-IRAQ)**

Vol.19, No.1, 2023 ***p 163 – 179***

THE EFFICIENCY OF SCS-CN, HEC-1, HEC-HMS, TR55, RATIONAL, AND SNYDER UNIT HYDROGRAPH MODELS FOR DETERMINING PEAK FLOOD DISCHARGE IN THE UPPER PART OF LESSER ZAB BASIN, KURDISTAN REGION, IRAQ

Fahmy O. Mohammed[1*], Diary A.M. Al-Manmi[1], and Ghafor A. Hamasur[1]

Received: 03/ 09/ 2022, Accepted: 08/ 01/ 2023
Keywords: Peak flood analysis; IGUH; SCS-CN model; Gumbel's method; Lesser Zab; Snyder Unit hydrograph

ABSTRACT

The Unit Hydrograph (UH) and Soil Conservation Service Curve Number (SCS-CN) are prevalent methods for estimating peak flow and peak time within the hydrological river basins. Different types of data, such as gauging data, morphometric analysis, and Land Use-Land Cover (LULC), are used to derive UH for the Kanarwe River Basin (KRB), which is an off-the-Lesser Zab River Basin (LZRB). Different hydrograph models, including HEC-1 (Hydrological Engineering Centre), TR55 (Technical release 55), HEC-HMS (Hydrological Engineering Centre-Hydrological Modeling System), Rational method, and Snyder unit hydrograph, have been applied and correlated with field data. Metrological data, geological setting, and land cover were integrated into the Geographic Information Systems (GIS) and Watershed Modelling System (WMS 11.1). The peak time (T*p*) and peak flow (Q*p*) were estimated based on the five applied models. The results for models are (Q*p* = 739.93 m^3/sec, T*p* = 20 hr), (Q*p* 181.4 m^3/sec, T*p* = 14 hr), (Q*p* = 800 m^3/sec, T*p* = 12 hr, (Q*p* = 341.13 m^3/sec, T*p* = 11.65 hr), (Q*p* = 443 m^3/sec, T*p* = 19.9 hr), (Q*p* = 243 m^3/sec) for HEC-1, TR55, HEC-HMS, Rational method, Synder unit hydrograph, and observed data respectively. The observed model (field data) peak time and peak flow value best agreed with the peak time and peak flow value of TR55, Snyder, and Rational models. Our finding confirmed that the geomorphoclimatic unit hydrograph, such as (Snyder) is highly efficient and more realistic for estimating peak time and peak flow for large basins than other models because it relates to basin characteristics.

INTRODUCTION

Sherman (1932), the first to propose the concept of a unit hydrograph, is "the direct runoff hydrograph produced by a unit volume of excess rainfall that is uniformly distributed over the drainage area and has a constant intensity". In flood-prone catchments, the peak flood discharge must be calculated from each watershed, and the appropriate size for any horological structure, such as a dam, must be specified (Jahangir *et al*., 2019; Suriya and Mudgal, 2012). Estimating and utilizing each hydrograph unit is vital, as all parameters influence channel flow size and peak flood formation (Bahrami *et al*., 2022; Sudhakar *et al*., 2015). Many assumptions and different models have been applied to draw and predict peak floods based on UH, such as the overall physical characteristics of the basin and constant

[1] Department of Geology, University of Sulaimani, Sulaymaniyah, Iraq,
*e-mail: fahmy.mohammed@univsul.edu.iq

effective rainfall independent of time (Silalahia and Hidayatb, 2019). Each method has advantages and disadvantages (Shaikh *et al*., 2022). The synthetic unit hydrograph (SUH) depends on the geomorphologic and climatic characteristics of the watershed (Tunas *et al*., 2019). Saeed *et al*. (2022) tried to estimate peak flow in the Lesser Zab based on climatological data and the soil and water assessment tool (SWAT) model; however, without any observed data within the basin. Rashid (2022) calculated the maximum and minimum surface runoff for Sulaimaniyah City based on CN-II and HEC-geoHMS model. This study aimed to first estimate peak flood and the peak time based on the HEC-1, HEC-HMS, Snyder model, TR55, Soil Conservation Service Curve Number (SCS-CN) method, and Rational method UH in KRB basin (Figure 1). Second, to compare model results with observed data to find which model is more acceptable. Finally, propose which models are more reliable for calculating peak flood and peak time in the Kanarwe watershed and Lesser Zab River Basin.

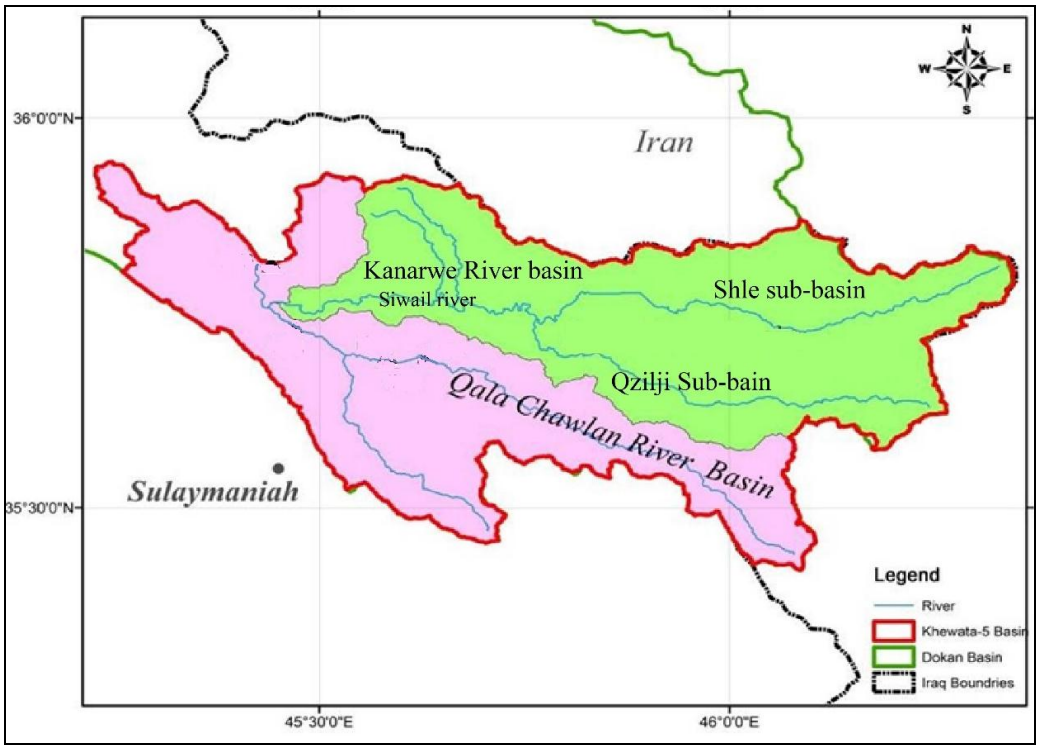

Figure 1: Shows Lesser Zab watershed, Kanawre River basin, and Qalachwlan River basin.

LOCATION

The Kanarwe River basin is a part of an enormous transboundary watershed called the Lesser Zab Basin (LZRB). It encompasses about 1542 Km^2 (Figure 1) within Sulaymaniyah province, Kurdistan region, Iraq. The climate in the area is semi-arid and cold, with an annual rainfall of 850 mm and an average temperature of 21 ^oC. A series of high mountains surround the watershed; the watershed's maximum and minimum heights are 2450 and 814 m a.s.l.

GEOLOGICAL SETTINGS

Tectonically, the study area is located within the Zagros mountain ranges (Haji Karim and Khanaqa, 2015; Jassim and Goff, 2006; Lawa *et al*., 2017) (Figure 2A). The Azmer anticline represents the main structural unit in this region; it has a general trend of Zagros (NW – SE). The upper part of the KRB, located within the Zagros Thrust Zone (ZTZ), is intensively deformed. The outcropped rock unit in the upper part of the KRB consists of

igneous rock of Mawat and Penjween, followed by Walash-Nawprda and Swais Group (Red bed series) (Buday, 1980) (Figure 2B). The lower part of the KRB ended with the northeast limb of the Azmer anticline, which consists of rocks of Aqra-Tanjero interfingering early cretaceous, and occasionally sinks downward the Zagros High Folded Zone, below the Swais Group (Paleogene-Red Bed Series) (Buday, 1980; Lawa *et al*., 2017) (Figure 2B).

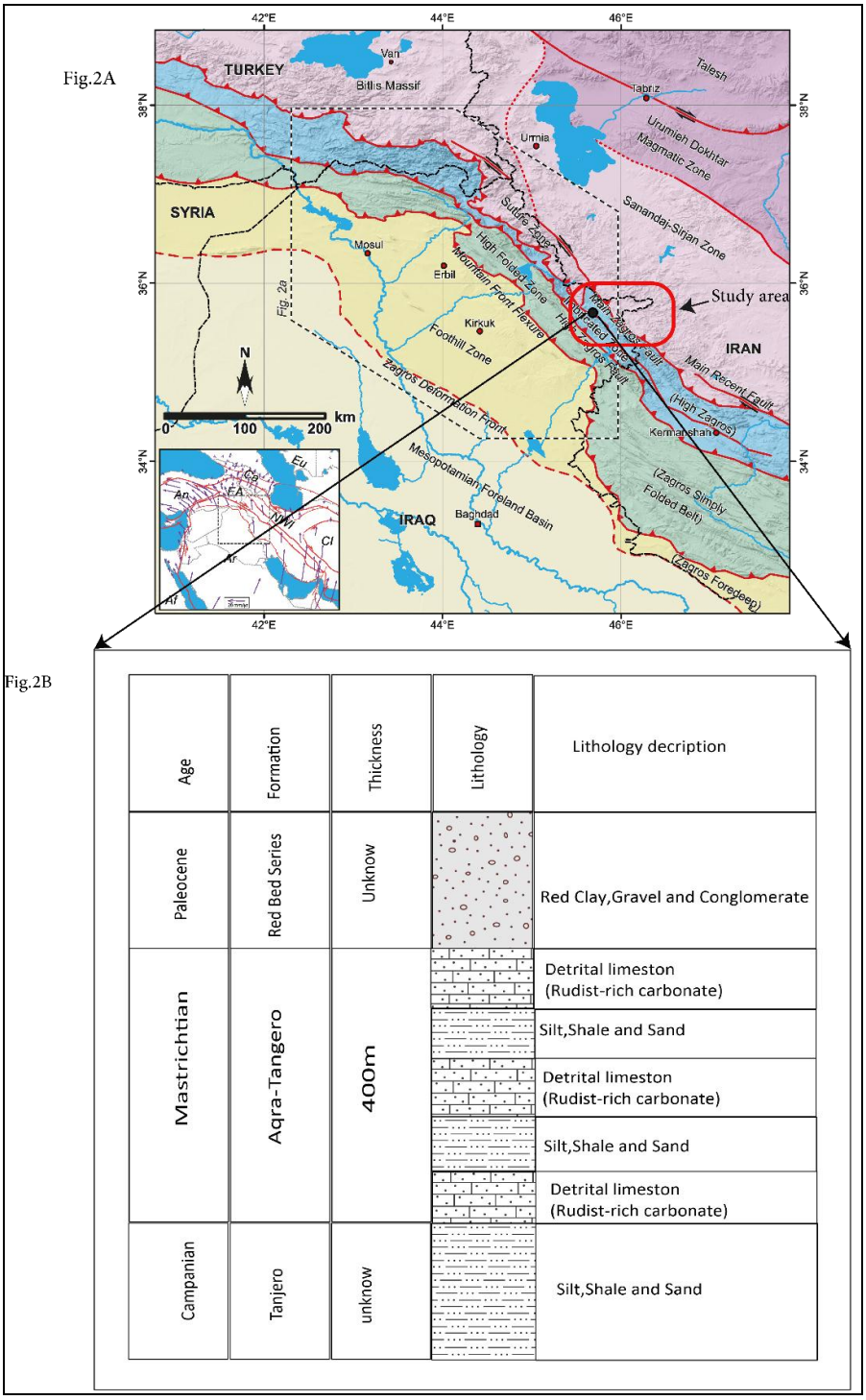

Figure 2: **A)** Regional tectonic setting of the study area (Zebari *et al*., 2020) and **B)** Stratigraphic column of the KRB outlet (black circle).

MATERIALS AND METHODS

A different hydrography model was applied in KRB to draw and calculate peak flood and peak time. ArcGIS10.8 and WMS 11.1 software were integrated with the different data sources to calculate UH parameters. The watershed delineation, water flow system and drainage characteristics were extracted from the Digital Elevation Model (DEM) 30 m resolution (Figure 3).

The morphometric results (Table 1), such as slope, length of the main river, area ratio (*R*A), bifurcation ratio (*R*B), and length ratio (*R*L) extracted from DEM based on Horton (1945); Strahler (1957). The Global Land Cover 10m resolution (Karra *et al*., 2021) was used for drawing the land cover map (Figure 4).

Food and Agriculture Organization of the United Nations (FAO) Soil maps (1: 500,000) (Latham *et al*., 2014) and land use land cover (LULC) were used for calculating the Curve Number (CN) value for each class of the LULC (Table 2), and the average weighted value (80.6) for CN-II for KRB (Figure 5).

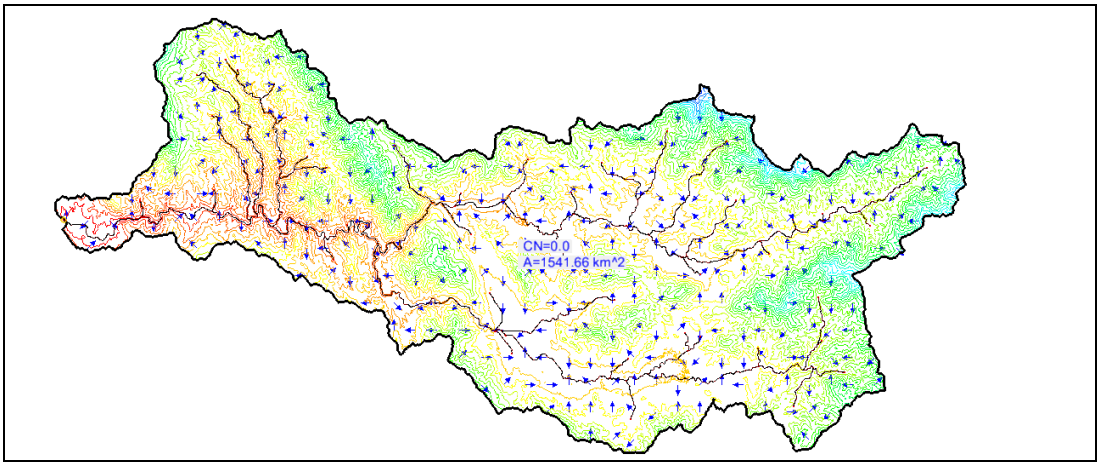

Figure 3: Shows water flow direction in the Kanarwe River Basin.

Table 1: Geomorphic parameters of Kanarwe River Basin.

No.	Morphometric Paramter	value	Unit
1	Average basin slope (BS)	0.2951	m/m
2	Basin length (L)	81202.88	M
3	Perimeter (P)	348889.44	M
4	*Curve number (CN)	80.6	
5	Shape Factor	4.23	mi^2/mi^2
6	Sinuosity (S)	1.511	MSL/l
7	Mean average basin elevation (AVEL)	1460.41	M
8	Max flow distance (MFD)	125313 m	M
9	Max flow slope (MFS)	0.0111	m/m
10	Max stream length (MSL)	122404.61	m
11	Max stream slope (MSS)	0.0078	m/m
12	Distance from the centroid to stream (CTOCTR)	630.83	m
13	Centeriod stream distance (CSD)	71964	m
14	Centeriod stream slope (CSS)	0.0053	m/m

***** CN is the weighted average value (See Table 2).

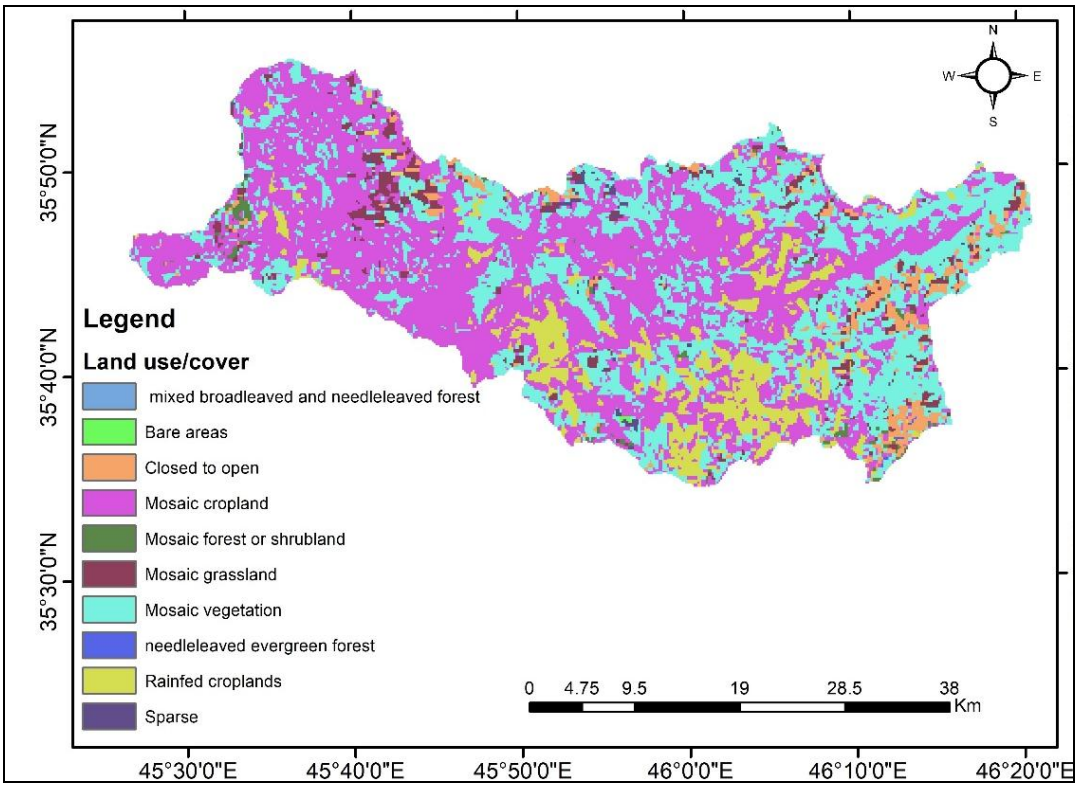

Figure 4: Land use map of the study basin.

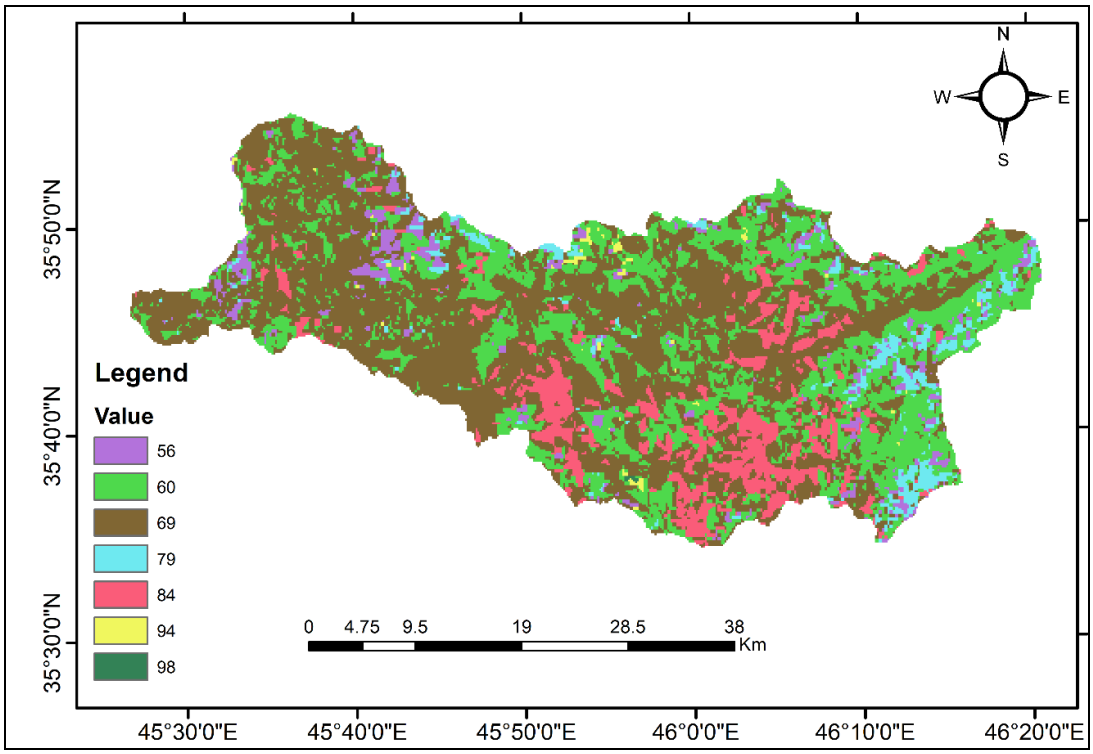

Figure 5: Curve number (CN) map of the study basin.

Table 2: LULC types and CN values.

Soil types	Land use description	CN code	Area (Km^2)	Product (CN x A)
*D	Sparse (< 15%) vegetation	94	481.359	45247.74
D	Closed to open (>15%) (broadleaved or needleless	77	21.111	1625.541
D	Rainfed croplands	84	72.466	6087.131
D	Mosaic vegetation (grass and/ shrubland/ forest)	79	114.837	9072.155
D	Mosaic forest or shrubland (50 – 70 %)/ grassland	77	22.009	1694.713
D	Mosaic cropland (50 – 70 %)/ vegetation (grassland)	84	123.072	10338.06
D	Bare areas	98	13.176	1291.21
D	Mosaic grassland (50 – 70 %)/ forest or shrubland	77	16.919	1302.738
D	Closed (> 40%) broadleaved deciduous forest (>5)	79	1.946	153.765
D	Closed (> 40%) needle-leaved evergreen forest	79	1.797	141.937
**B	Sparse (< 15%) vegetation	86	181.614	15618.79
B	Mosaic vegetation (grassland/ shrubland/ forest)	60	120.227	7213.646
B	Mosaic grassland (50 – 70 %) / forest or shrubland	56	39.826	2230.271
B	Mosaic cropland (50 – 70 %)/ vegetation (grassland)	69	105.105	7252.274
B	Rainfed croplands	69	155.562	10733.78
B	Closed to open (> 15%) (broadleaved or needleless	56	22.758	1274.441
B	Mosaic forest or shrubland (50 – 70 %) / grassland	56	37.131	2079.351
B	Bare areas	98	12.277	1203.173
B	Closed (> 40%) broadleaved deciduous forest (>5)	60	5.689	341.368
CN	(Weighted) = Total Product\ Total Area	80.6		

*****D (clay loam; silty clay; clay; sandy clay); ******B (Loam; silt loam) ("FAO Map Catalog," n.d.; "Harmonized World Soil Database v1.2 | FAO SOILS PORTAL | Food and Agriculture Organization of the United Nations," n.d.)

- **Hydrological Model**

Estimation of peak flow and the peak time for any ungagged watershed is based on two approaches, which include:

– **First:** Estimating excess rainfall using the Soil Conservation Service (SCS) method (Figure 6). Excess rainfall is the percentage of rainfall that becomes direct runoff after accounting for infiltration and other losses (Adnan *et al*., 2021; Ehsan *et al*., 2021). Excess rainfall can be estimated using the equation:

$$Q = \frac{(P \pm Ia)2}{(P - Ia) + S} \quad \text{..... Eq.1}$$

Where P is the total rainfall, S is the maximum potential retention after runoff begins, and Ia is the initial abstraction = 0.2 S (Service, 1986).

– **Second:** Estimating surface runoff (peak flow and peak time) using synthetic unit hydrographs. A unit hydrograph (UH) is a direct runoff hydrograph. (i.e., excluding base flow) (Figure 7).

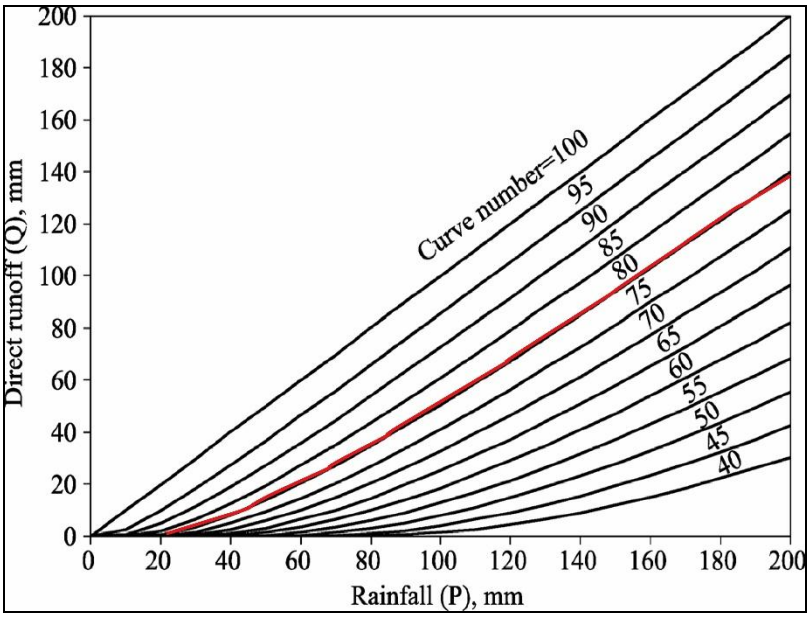

Figure 6: Basic SCS rainfall-runoff relationship for different CN values (Service, 1986), and the red line represents the CN value for the study area.

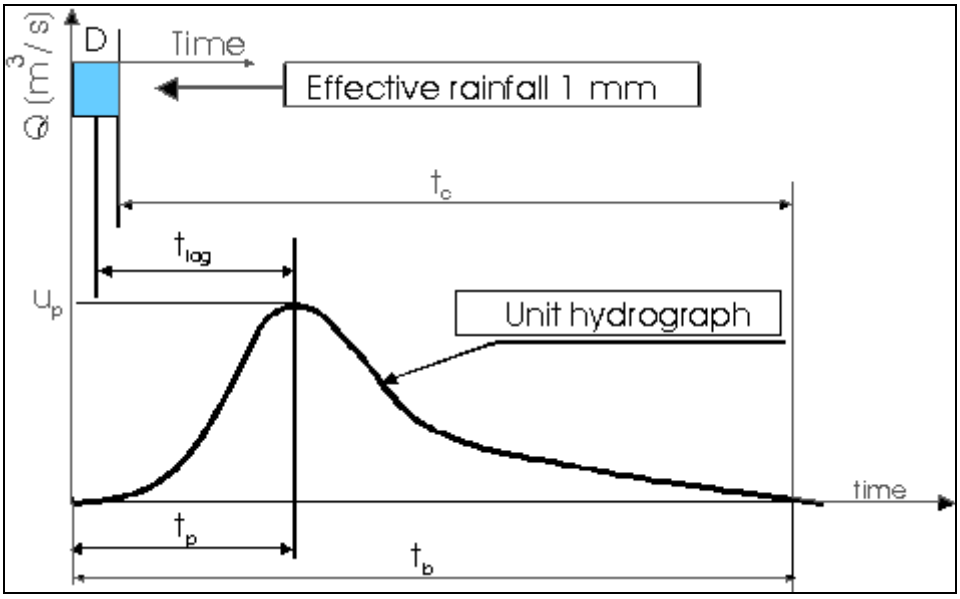

Figure 7: Characteristics of the unit hydrograph (Service, 1986).

- **The Synthetic SSC Unit Hydrograph**

The SCS, US Department of Agriculture, employs an average number of natural SUH for watersheds that vary significantly in size and geographical location (Nourani *et al*., 2009). In deriving the flood hydrograph, this theory has been regarded as an essential contribution to the field of hydrology (Yi *et al*., 2022). However, due to limiting assumptions, UH theory limits precise runoff prediction (Sudhakar *et al*., 2015). The SCS model permits computing the UH for a watershed with insufficient observed rainfall-runoff data (Chow *et al*., 1988). The lag time Tl in the SCS model will be determined using watershed physical properties such as main river length, average slope, and CN (Khaleghi *et al*., 2011; Muleta *et al*., 2022; Pal and Samanta, 2011).

The CN was determined using land use and soil hydrological group maps in different antecedent moisture conditions (dry, average, and moist) and hydrological conditions (Krisnayanti *et al*., 2021; Mukherjee *et al*., 2021). The total of soil and surface interception, infiltration, and transmission is used to estimate loss (mm), and the runoff calculation steps are given below:

$$Q = \frac{(P - 0.2S)^2}{P - 0.8S} \ldots\ldots\ldots\ldots\ldots\ldots\ldots\ldots\ldots\ldots\ldots\ldots\ldots\ldots \text{Eq. 2}$$

Where,
Q = depth of direct runoff (mm)
P = depth of rainfall for a specific return period (mm)

The CN was calculated using land use and maps of soil hydrological groups in the basin's moderate antecedent moisture conditions (type II 24 hr) (Fischer *et al*., 2008; Latham *et al*., 2014). Then, losses S were calculated (in mm) using Eq.3

$$S = (25400 / CN) - 254 \ldots\ldots\ldots\ldots\ldots\ldots\ldots\ldots\ldots\ldots \text{Eq.3}$$

The maximum flood discharge was calculated using Eq.4 for calculating storm runoff:

$$Qmax = 2.083AQ/tp \ldots\ldots\ldots\ldots\ldots\ldots\ldots\ldots\ldots\ldots \text{Eq.4}$$

Qmax is maximum flood discharge (m^3/s), A is basin area (km^2), Q is runoff (mm), Tp is the time of flood crest, which is evaluated by the time of concentration, and tc is in a minute.

The lag time *t*L(h) and time to peak *t*P (h) were calculated using the following formulas:

$$tL = \frac{L^{0.8}(S+1)^{0.7}}{1900Y^{0.5}} \ldots\ldots\ldots\ldots\ldots\ldots\ldots\ldots\ldots\ldots\ldots\ldots \text{Eq.5}$$

$$tp = \frac{D}{2} + tL(D = 0.133tc) \ldots\ldots\ldots\ldots\ldots\ldots\ldots\ldots\ldots\ldots \text{Eq.6}$$

Where L is the main river length (m), S is the average slope (%), D is the period of rainfall (h), and *t*c is the time of concentration (h) (Sultan *et al*., 2022).

RESULTS

A single rainfall-runoff event with no melting snow was chosen for the analysis. Rainfall was recorded daily, but discharge data were collected monthly from the Sulaymaniyah Irrigation Directorate. Peak flow and peak time were calculated using a statistical approach from historical data and five hydrological models. Using six different models, WMS v.11.1 was used to estimate peak flow and the peak time in the KRB.

- **HEC-1 AND TR55**

A single storm event lumped parameter model includes several basin parameters, such as rainfall options, losses, unit hydrographs, and stream routing. The HEC-1 and TR55 packages, data entering, and display analysis results are very instances within WMS. The input parameter was 61 mm rainfall for 24 hr, and the type II SCS method was applied. The peak flow and peak time was (Q*p* = 739.93 m^3/sec, T*p* = 20 hr) for HEC1, (Q*p* = 181.4 m^3/sec, T*p* = 14 hr) for TR55 (Figures 8A and 8B).

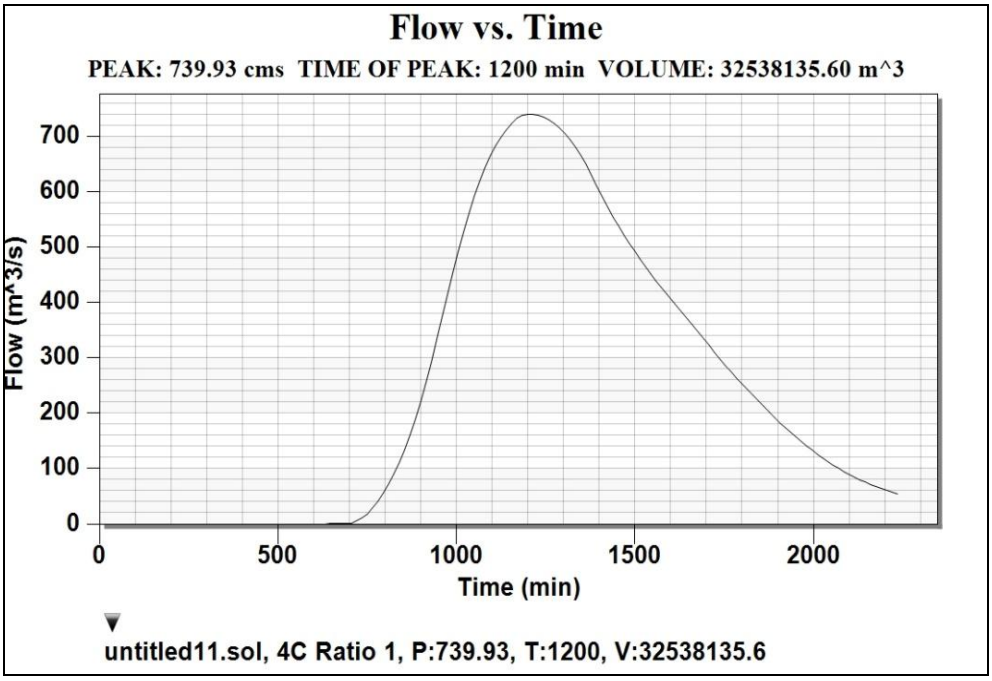

Figure 8A: HEC-1 model estimation of the peak of flow and time of peak for the KRB.

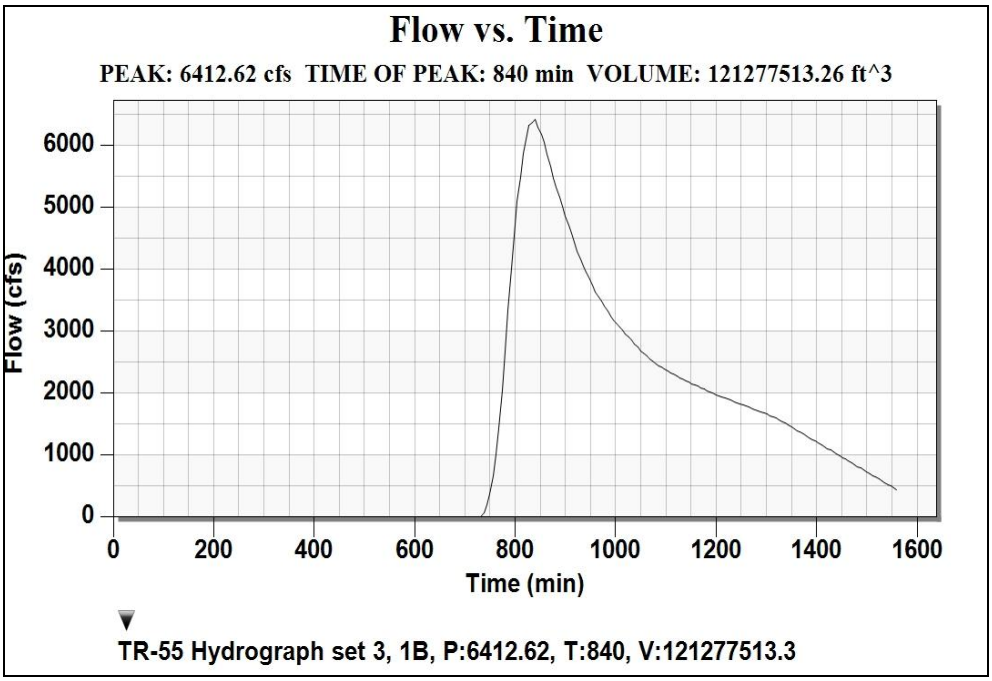

Figure 8B: Estimating the peak of flow and peak time for the KRB
by the TR55 model.

- **HEC-HMS**

HEC-HMS intends to replace HEC-1 as it uses the same input as HEC-1 but adds additional capabilities, including the MODClark quasi-distributed (2D) hydrologic model, precipitation loss estimation, and outflow. Using the Same input parameter, 61 mm rainfall for 24 hr, and the types II SCS method and applying types three methods. The peak flow and peak time were (Qp = 800 m^3/sec, Tp = 12 hr) (Figure 9).

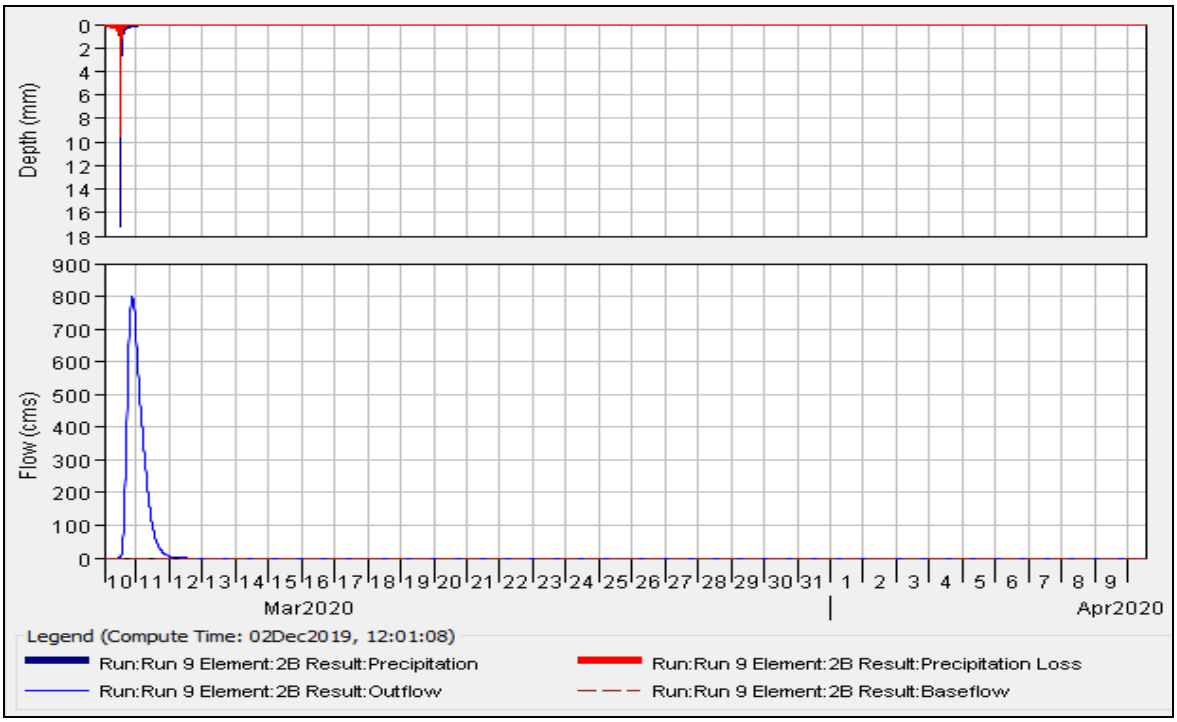

Figure 9: HEC-HMS model estimation peak of flow, base flow, and ppt loss in the KRB.

- **The Rational**

In engineering hydrology, the rational method is widely used; however, it only applies in urban areas and produces results with significant uncertainty (McKerchar and Macky, 2001). The Rational Formula (RF) calculates peak flow and time (Baiamonte, 2020).

The Rational Method formula can be written as follow:

$$Q = CiA \quad \text{..... Eq.7}$$

Where: Q is peak discharge, C is runoff coefficient, i is precipitation intensity, and A is catchment area.

The C value is partly chosen in any catchment based on physiographic conditions, engineering judgment, and rainfall intensity (Itsukushima, 2019). The rational formula predicts surface runoff (Erena and Worku, 2019). (Q = CiA/3.6); the critical point is that both i and C must be evaluated depending on the climatic condition of the selected watershed. WMS software uses the CN value to calculate the rainfall coefficient. Based on terrain conditions, a high mountainous slope is 30%, and land cover types are vegetation; the C value is 0.3 (Tsutsumi *et al*., 2004). The peak flow and peak time were (Qp = 341.13 m^3/sec, Tp = 11.8 hr) (Figure 10).

- **Snyder Unit Hydrograph (Suh)**

Synder (1938) developed a set of empirical equations for synthetic unit hydrograph (SUH) in many catchments in the eastern United States' Appalachian Highland (Figure 11). Unlike Sherman's Unit Hydrograph method, the SUH method has better acceptability for ungauged basins, large river basins of more than 25 Km^2.

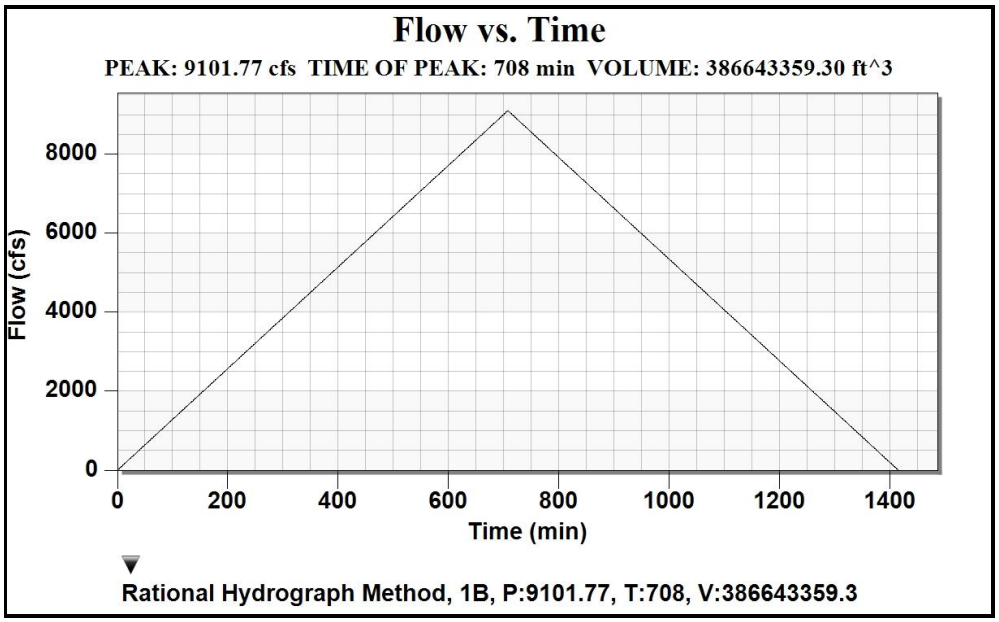

Figure 10: Rational model estimation of peak flow and time concentration in the KRB.

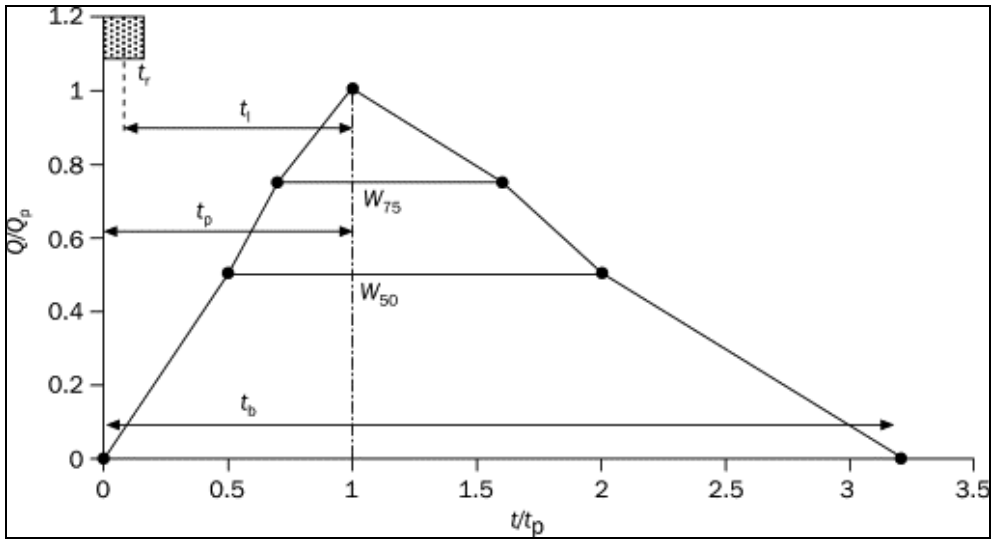

Figure 11: Synder synthetic unites hydrograph (Snyder, 1938).

The constant Cw_{75} is 1.22 for the 75% width, and Cw_{50} *is* equal to 2.14 for the 50% width. Hence, it is possible to develop the shape, standard time lag, time base, time of the peak, and peak discharge of each sub-watershed.

Since KRB has a drainage area of 1542 Km^2, the length of the mainstream is 122 Km, and the main channel length from the watershed outlet to the point opposite the center of gravity of the watershed is 71 Km; using C_1 = 0.75, C2 = 2.75, C_3=5.56 C_t = 0.4 and C_p = 0.625, determine the SUH for this basin.

Step 1 ------- Standard rainfall duration, $t_r = t_p / 5.5 = 5.96 / 5.5 = 1.08$ hr, $tr \neq t_R$.

Step 2 ------- $t_p = C_1 C_t (LL_c)^{0.3} = 0.75 \times 0.4 (122 \times 71)^{0.3} = 5.96$ hr

Step 3 ------- $Q_p = \frac{C2*A*C_p}{(t_p)}$ = 1542 × 2.75 x 0.625/3.85 = 444 m^3/s

Step 4 ------- $t_{pr} = t_p - (t_r - t_R)/4$ = 5.96 – (1.08 – 0.5)/ 4 = 5.89 hr

Step 5 ------- $Q_{pR} = Q_p \times Tp/t_{pr}$ = 444 × 5.96/ 5.89 =449 m^3/s

Step 6 ------- $t_b = C_3*A/ Q_{pR}$ = 5.56 × 1542/ 449 = 19.09 hr

Widths in the hour of unit hydrograph at discharge equal to a certain percent of peak discharge ($Q_{PR)}$ given by

$$W_{75} = \frac{C_{75}}{(Q_{pR}/A)^{1.08}} = \frac{1.22}{(449/1542)^{1.08}} = 4.6\ hr$$

$$W_{50} = \frac{C_{50}}{(Q_{pR}/A)^{1.08}} = \frac{2.14}{(449/1542)^{1.08}} = 8.26\ hr$$

The C_t coefficient represents variations in watershed slopes and storage characteristics. C_p is the peak coefficient representing the effects of retention and storage. (W%) are relationships for the widths of the UH at values of 50% (*W50*) and 75% (*W75*).

- **Peak Flood Calculation Using Gumbel Statistical Approach**

Data from (2011 to 2015) on average monthly peak flow was obtained for Sulaymaniyah Irrigation Directorate (Table 3). This observed data is critical and is used for calculating the mean annual peak flood discharge based on the statistical approach of Gumbel's Method (Fischer *et al*., 2008; Latham *et al*., 2014).

Table 3: Show the discharge of the KRB.

Years	Stream flow peak annual (m^3/sec)	Flood peak in descending (m^3/sec)	order
2011	83.854	124.3817	1
2012	124.3817	101.0266	2
2013	14.298	83.854	3
2014	48.786	48.786	4
2015	101.0266	14.298	5
SUM	372.3463	Yt	4.600149
Average($\bar{x}$)	74.46926	$\bar{y}n$	0.485
Standard deviation σ_n	0.91		

Based on the Gummble equation, the peak of the Annual flood 100-year interval was estimated based on the following equations:

$$yt = -Ln\{Ln(T)\}/ Ln(T-1) \quad \text{..... Eq.8}$$

where yt is the return interval, T = time interval (2, 5, 10, 100) years,

$$K = (Yt - \bar{y}n)\ Sn \quad \text{..... Eq.9}$$

Where K is frequency factor 4.3227, $\bar{y}n$ = Reduce mean 0.485 from Gumble extreme value, Sn = reduce stander deviation0.91.

The values of ȳn and Sn are selected from Gumbel's Extreme Value Distribution and considered depending on the sample size

$$Xt = \bar{x} + (k \times \sigma) \text{ ..... Eq.10}$$

Xt the peak of the annulling river at recurrent interval 100

$\bar{x}$ = average annual peak discharge, σ_{n-1} = Stander deviation for sample size, Xt = 262.4798643 m^3/sec (Table 4).

Table 4: Peak flood different time intervals.

No.	Time interval (T)	Frequency factor(K)	Peak stream flow(m3/sec)
1	2	− 0.1355	68.5
2	5	1.0580	120
3	10	1.8483	154.8
4	100	4.3227	270.4

DISCUSSION

Different unit hydrograph models and morphometric analyses were applied to calculate peak floods in KRB. Estimating these models' parameters depends mainly on the site's DEM, satellite images, LULC, Soil map, and digital electronic-gauging station. The DEM control was the most geomorphic parameter, while land use and soil types controlled the CN values. The software packages also control all models' outputs, depending on the algorithm behind all software. The end-user must decide which one is best for the selected basin. It also depends on the data availability, limitations, and assumptions that control each model (Table 5).

Table 5: Summary of methods for estimating flood hydrograph in the KRB.

Models	Description	Advantages	Disadvantages	Data requirements	Q_{peak} *and* T_{peak}
HEC-1	Single event	A relatively simple approach	limited to gauged catchments	Storm hyetograph	*Qp* = 739.93 m^3/sec *Tp* = 20 hr
TR55	Single event	A relatively simple approach	They are used for the small basin.	Storm Hyetograph	*Qp*=181.1m^3/sec *Tp=14hr*
HEC-HMS	The empirical approach that converts a hyetograph into a hydrograph	A relatively simple approach	It is limited to gauged catchments	Storm hyetograph.	*Qp* = 800 m^3/sec *Tp* = 12 hr
Rational method	An empirical method to estimate peak flow and peak time	The calculation is straightforward and most preferable for engineers	Not applicable when rainfall varies significantly across the catchment;	runoff coefficient, which depends on catchment characteristics	*Qp* = 341.13 m^3/sec *Tp* = 11.65 hr
Snyder Unit Hydrograph	the empirical method to estimate peak flow and time peak	better acceptability for ungauged basins	Limited for small watersheds less than 25 Km^2	Basin morphology, geometry,	*Qp* = 443 m^3/sec *Tp* = 19.9 hr
Gumbel's Method	the empirical equation	Required observed data	Statistical approaches	Depending on the annual discharge measurement	Qp_{annual} = 262.5 m^3/sec

The models simulate the data, drawing each type's resulting hydrographs (Figures 8, 9, and 10). In the end, all models are compared with each other and observed data. The comparison confirmed that all models' runoff volume results are either lower or higher than the observed annual peak flow. This variation has come from the models taking single-event rainfall as input, but the observation data is multi-event rainfall. The result of HEC1 (739 m^3/sec) and HEC-HMS (800 m^3/sec) coincides with (Rashid, 2022), which is 794.98 m^3/sec). While TR55, Rational, and Synder results coincide with those (Saeed *et al*., 2022), which are between (180 to 450 m^3/sec).

This high-value Q*p* and T*p* are strongly related to CN value. The high value of CN 80.6 affects the results of all model outputs, which reflect the high percentage of surface runoff and low groundwater recharge because of the high topography, steep slope, and outcrop igneous rock in most of the basin (Nageswara Rao, 2020).

All input data unified to a single event and 61 mm rainfall and CN value of 80.6; all models failed to simulate the same value for peak flow (Q*p*) and peak time (T*P*) because of different assumptions behind each model. It should be noted that these models may contain errors because the experimental equations were derived based on catchment datasets in other climate conditions around the world and vailed for a specific region. Many researchers agree with the results of Snyder, and SCS models could better estimate because these two models work more with geographic location, climatic data, and geomorphic parameters (Hoffmeister and Weisman, 1977; Nourani *et al*., 2009; Zakizadeh and Malekinezhad, 2015). Climate change affects selected basins (Mohammed *et al*., 2021). This led to uncertainty in those models that work just on meteorological characteristics, such as HEC-1, TR55, HEC-HMS, and Rational Models.

CONCLUSION

Different models were applied to estimate peak flood discharge and peak time within KRB, NE of Iraq. The WMS software and ArcGIS were used to calculate and run all hydrological models, including HEC-1, TR55, HEC-HMS, Rational, and Snyder. The results of HEC-1 and HEC-HMS models gave similar results, while the results from TR55, Rational, and Synder were lower than those from HEC-1 and HEC-HMS. Comparing UH model results with observed data (Gumbel Approach) reveals that Snyder, rational, and TR55 are more accurate since they relate to the empirical equation and statistical approach. The result also showed that morphometric analysis controls the shape of UH, especially Snyder unit hydrographs. As a result, it is suggested that similar formulae could be developed for corresponding regions in Iraq and subsequently applied to other watersheds with similar morphological scenarios. Implementing this recommendation is difficult in developing countries such as Iraq, where data shortages and severe climate changes are expected. The research concludes that applying Snyder and SCS models provides better estimation for the base time parameters than the other three models because these two models work with geographic location and climatic data compared with other models.

Thus, it is not advisable to suggest these models for the estimation of peak flow and the peak time of watersheds with similar conditions without more investigation, especially for large catchments like Lesser Zab, which consist of many sub-basins, and each sub-basin has its climate conditions, vegetation cover, and different land covers.

ACKNOWLEDGEMENT

The authors express their deep sense of thankfulness to USGS and FAO for the free data used in this study. Also, we would like to thank the Sulaymaniyah Irrigation Directorate, especially Mr. Ari Ismail, the Head of the Surface Water department, for providing river discharge data of the study area for Free. We appreciate Dr. Anwar O. Mohammed from the University of Sulaimani, Sulaymaniyah, Iraq, for editing the manuscript's language.

REFERENCE

Adnan, R.M., Petroselli, A., Heddam, S., Santos, C.A.G. and Kisi, O., 2021. Short term rainfall-runoff modeling using several machine learning methods and a conceptual event-based model. Stochastic Environmental Research and Risk Assessment, Vol.35, No.3, p. 597 – 616.

Bahrami, E., Salarijazi, M. and Nejatian, S., 2022. Estimation of flood hydrographs in the ungauged mountainous watershed with Gray synthetic unit hydrograph model. Arabian Journal of Geosciences, Vol.15, No. 8, p. 1 – 10.

Baiamonte, G., 2020. A rational runoff coefficient for a revisited rational formula. Hydrological Sciences Journal, Vol.65, No.1, p. 112 – 126.

Buday, T., 1980. Regional Geology of Iraq, Vol.1 Stratigraphy. In: Kassab, I.I. and Jassim, S.Z. (Eds.). GEOSURV, Baghdad, 445pp.

Chow, V.T., Maidment, D.R. and Larry, W., 1988. Mays. Applied Hydrology. International Edition, MacGraw-Hill, Inc, 149pp.

Ehsan, M.A., Tippett, M.K., Robertson, A.W., Almazroui, M., Ismail, M., Dinku, T., …, and Teshome, A., 2021. Seasonal predictability of Ethiopian Kiremt rainfall and forecast skill of ECMWF's SEAS5 model. Climate Dynamics, Vol.57, No.11, p. 3075 – 3091.

Erena, S.H. and Worku, H., 2019. Dynamics of land use land cover and resulting surface runoff management for environmental flood hazard mitigation: The case of Dire Daw city, Ethiopia. Journal of Hydrology: Regional Studies, 22, 100598.

FAO Map Catalog. (n.d.). Retrieved October 10, 2021, from https://data.apps.fao.org/map/catalog/srv/eng/catalog.search#/metadata/ba4526fd-cdbf-4028-a1bd-5a559c4bff38

Fischer, G., Nachtergaele, F., Prieler, S., Van Velthuizen, H., Verelst, L. and Wiberg, D., 2008. Global agro-ecological zones assessment for agriculture (GAEZ 2008). IIASA, Laxenburg, Austria and FAO, Rome, Italy, 10pp.

Haji Karim, K. and Khanaqa, P.A., 2015. Association of rudists and red clastic facies in the upper part of Aqra Formation, Mawat area, Kurdistan Region, NE Iraq. Arabian Journal of Geosciences, Vol.8, No.5, p. 2751 – 2759.

Harmonized world soil database v1.2 | FAO SOILS PORTAL | Food and Agriculture Organization of the United Nations. (n.d.). Retrieved October 7, 2021, from http://www.fao.org/soils-portal/data-hub/soil-maps-and-databases/harmonized-world-soil-database-v12/en/

Hoffmeister, G. and Weisman, R.N., 1977. Accuracy of Synthetic Hydrographs Derived from Representative Basins/La précision des hydrogrammes synthétiques dérivés des bassins représentatifs. Hydrological Sciences Journal, Vol.22, No.2, p. 297 – 312.

Horton, R.E., 1945. Erosional development of streams and their drainage basins; hydrophysical approach to quantitative morphology. Geological Society of America Bulletin, Vol.56, No.3, p. 275 – 370.

Itsukushima, R., 2019. Characteristics and controlling factors of the drought runoff coefficient. Hydrology and Earth System Sciences Discussions, p. 1 – 24.

Jahangir, M.H., Reineh, S.M.M. and Abolghasemi, M., 2019. Spatial prediction of flood zonation mapping in Kan River Basin, Iran, using artificial neural network algorithm. Weather and Climate Extremes, 25, 100215.

Jassim, S.Z. and Goff, J.C., 2006. Geology of Iraq. DOLIN, sro, distributed by Geological Society of London.

Karra, K., Kontgis, C., Statman-Weil, Z., Mazzariello, J.C., Mathis, M. and Brumby, S.P., 2021. Global land use/ land cover with Sentinel 2 and deep learning. p. 4704 – 4707. IEEE.

Khaleghi, M.R., Gholami, V., Ghodusi, J. and Hosseini, H., 2011. Efficiency of the geomorphologic instantaneous unit hydrograph method in flood hydrograph simulation. Catena, Vol.87, No.2, p. 163 – 171.

Krisnayanti, D.S., Bunganaen, W., Frans, J.H., Seran, Y.A. and Legono, D., 2021. Curve number estimation for ungauged watershed in semi-arid region. Civil Engineering Journal, Vol.7, No.6, p. 1070 – 1083.

Latham, J., Cumani, R., Rosati, I. and Bloise, M., 2014. Global land cover share (GLC-SHARE) database beta-release version 1.0-2014. FAO: Rome, Italy.

Lawa, F.A., Al-Karadakhi, A.I. and Ismail, K.M., 2017. An interfingering of the Upper Cretaceous rocks from Chwarta–Mawat Region, NE Iraq. Iraqi Bulletin of Geology and Mining, Vol.13, No.1, p. 15 – 26.

McKerchar, A.I. and Macky, G.H., 2001. Comparison of a regional method for estimating design floods with two rainfall-based methods. Journal of Hydrology (New Zealand), p. 129 – 138.

Mohammed, F.O., Mohammad, A.O., Ibrahim, H.S. and Hasan, R.A., 2021. Future Scenario of Global Climate Map change according to the Köppen-Geiger Climate Classification. Baghdad Science Journal, Vol.18, No.2, (Suppl.), p. 1030 – 1030.

Mukherjee, P., Das, A. and Das, R., 2021. Determination of SCS Runoff Curve Number and Landuse Characteristics of Khowai River Catchment, Tripura, India. In Sustainability in Environmental Engineering and Science, p. 167–173. Springer.

Muleta, B., Seyoum, T. and Assefa, S., 2022. GIS-Based Assessment of Suitability Area of Rainwater Harvesting in Daro Labu District, Oromia, Ethiopia. American Journal of Water Science and Engineering, Vol.8, No,1, p. 21 – 35.

Nageswara Rao, K., 2020. Analysis of surface runoff potential in ungauged basin using basin parameters and SCS-CN method. Applied Water Science, Vol.10, No.1, p. 1 – 16.

Nourani, V., Singh, V.P. and Delafrouz, H., 2009. Three geomorphological rainfall–runoff models based on the linear reservoir concept. Catena, Vol.76, No.3, p. 206 – 214.

Pal, B. and Samanta, S., 2011. Surface runoff estimation and mapping using remote sensing and geographic information system. Int. J. Adv. Sci. Technol, Vol.3, No.2, p. 106 – 114.

Rashid, H.M., 2022. GIS Based Surface Runoff Estimation for Sulaimani City, KRG, Iraq. Association of Arab Universities Journal of Engineering Sciences, Vol.2, p. 35 – 46.

Saeed, F.H., Al-Khafaji, M.S. and Al-Faraj, F.A., 2022. Spatiotemporal hydroclimatic characteristics of arid and semi-arid river basin under climate change: A case study of Iraq. Arabian Journal of Geosciences, Vol.15, No.14, p. 1 – 12.

Service, S.C., 1986. Urban hydrology for small watersheds. Technical Release No., 2.5 – 2.8.

Shaikh, M.P., Yadav, S.M. and Manekar, V.L., 2022. Assessment of the empirical methods for the development of the synthetic unit hydrograph: A case study of a semi-arid river basin. Water Practice and Technology, Vol.17, No.1, p. 139 – 156.

Sherman, L.K., 1932. Streamflow from rainfall by the unit-graph method. Eng. News Record, Vol.108, p. 501 – 505.

Silalahia, F. and Hidayatb, F., 2019. Modelbuilder and Unit Hydrograph for Flood Prediction and Watershed Flow Direction Determination at The West Branch of The Little River, Stowe, Lamoille County, Vermont, USA. Geoplanning: Journal of Geomatics and Planning, Vol.6, No.2, p. 89 – 98.

Snyder, F.F., 1938. Synthetic unit-graphs. Eos, Transactions American Geophysical Union, Vol.19, No.1, p. 447 – 454.

Strahler, A.N., 1957. Quantitative analysis of watershed geomorphology. Eos, Transactions American Geophysical Union, Vol.38, No.6, p. 913 – 920.

Sudhakar, B.S., Anupam, K.S. and Akshay, O.J., 2015. Snyder unit hydrograph and GIS for estimation of flood for un-gauged catchments in lower Tapi basin, India. Hydrology: Current Research, Vol.6, No.1, 1pp.

Sultan, D., Tsunekawa, A., Tsubo, M., Haregeweyn, N., Adgo, E., Meshesha, D.T., …, and Setargie, T.A., 2022. Evaluation of lag time and time of concentration estimation methods in small tropical watersheds in Ethiopia. Journal of Hydrology: Regional Studies, 40, 101025.

Suriya, S. and Mudgal, B., 2012. Impact of urbanization on flooding: The Thirusoolam sub watershed–A case study. Journal of Hydrology, Vol.412, p. 210 – 219.

Tsutsumi, A., Jinno, K. and Berndtsson, R., 2004. Surface and subsurface water balance estimation by the groundwater recharge model and a 3-D two-phase flow model/Estimation de bilan hydrologique de surface et de subsurface à l'aide de modèles de recharge de nappe et d'écoulement diphasique 3-D. Hydrological Sciences Journal, Vol.49, 2pp.

Tunas, I.G., Anwar, N. and Lasminto, U., 2019. A synthetic unit hydrograph model based on fractal characteristics of watersheds. International Journal of River Basin Management, Vol.17, No.4, p. 465 – 477.

Yi, B., Chen, L., Zhang, H., Singh, V.P., Jiang, P., Liu, Y., Guo, H. and Qiu, H., 2022. A time-varying distributed unit hydrograph method considering soil moisture. Hydrology and Earth System Sciences, Vol.26, No.20, p. 5269 – 5289.

Zakizadeh, F. and Malekinezhad, H., 2015. Comparison of methods for estimation of flood hydrograph characteristics. Russian Meteorology and Hydrology, Vol.40, No.12, p. 828 – 837.

Zebari, M., Balling, P., Grützner, C., Navabpour, P., Witte, J. and Ustaszewski, K., 2020. Structural style of the NW Zagros Mountains and the role of basement thrusting for its Mountain Front Flexure, Kurdistan Region of Iraq. Journal of Structural Geology, 141, 104206.

About the author

Fahmy Osman Mohammed graduated from the University of Sulaimani in 2005 with a B.Sc. in Geology. He was awarded M.Sc.degrees in 2011 from the same university in Engineering geology. He is a Ph.D. student in the Geology Department at the University of Sulaimani. He has 15 years of experience in Engineering Geology, Environmental modeling, Remote sensing, and GIS. He has five published articles on different geological aspects.

e-mail: fahmy.mohammed@univsul.edu.iq